Solid State Electronics 144 (2018) 67–72

Contents lists available at ScienceDirect

Solid State Electronics

journal homepage: www.elsevier.com/locate/sse

A charge-based model of Junction Barrier Schottky rectifiers

Alvaro D. Latorre-Rey[a,*], Mihir Mudholkar[b], Mohammed T. Quddus[b], Ali Salih[b]

[a] School of Electrical, Computer and Energy Engineering, Arizona State University, Tempe, AZ 85287, USA
[b] Power Solutions Group, ON Semiconductor, 5005 E McDowell Rd, Phoenix, AZ 85008, USA

ARTICLE INFO

The review of this paper was arranged by Prof. A. Zaslavsky

Keywords:
Junction Barrier Schottky
Rectifiers
Breakdown voltage
Compact modeling

ABSTRACT

A new charge-based model of the electric field distribution for Junction Barrier Schottky (JBS) diodes is presented, based on the description of the charge-sharing effect between the vertical Schottky junction and the lateral pn-junctions that constitute the active cell of the device. In our model, the inherently 2-D problem is transformed into a simple but accurate 1-D problem which has a closed analytical solution that captures the reshaping and reduction of the electric field profile responsible for the improved electrical performance of these devices, while preserving physically meaningful expressions that depend on relevant device parameters. The validation of the model is performed by comparing calculated electric field profiles with drift-diffusion simulations of a JBS device showing good agreement. Even though other fully 2-D models already available provide higher accuracy, they lack physical insight making the proposed model an useful tool for device design.

1. Introduction

Power rectifiers constitute an essential component in widespread applications driven by the automotive, consumer electronics and communication industries. Traditionally, the planar Schottky rectifier technology has satisfied the demand for high efficiency and low cost devices, however as power and frequency requirements become more demanding, the limitations of planar rectifiers have become prohibitive in terms of electrical performance: the forward voltage drop increases super-linearly when increasing breakdown voltage, and the reverse leakage current increases exponentially with temperature, because drift regions are made thicker and doped lighter [1]. The Junction Barrier Schottky (JBS) [2], recently demonstrated in wide-bandgap materials such as SiC and GaN [3,4], has become a good alternative to overcome the planar Schottky limitations. The JBS consists of a Schottky barrier diode with a pn-junction grid placed directly under the metal, designed to allow forward voltage conduction while creating a potential barrier under reverse bias that shields the Schottky contact allowing higher blocking voltages and lower leakage currents [5].

Even though several highly accurate 2-D models have been proposed for JBS rectifiers [6,7], their approach yields rather complicated mathematical expressions for the electric field which mask the operating principles of the device and the physical meaning of relevant design parameters. In this work, we present a simple but accurate model for the electric field of JBS diodes based on the description of the charge-sharing effect between the vertical Schottky junction and the lateral pn-junctions that constitute the active cell of the device, transforming the 2-D problem into a 1-D model that yields simple expressions while preserving the physical meaning of relevant design parameters. First the charge-sharing effect is used to provide a qualitative explanation of operating principles of JBS devices, then the model equations are derived and validated with drift-diffusion simulations. Even though this analysis is presented on Si devices, the concepts apply for other materials such as SiC and GaN.

2. Charge-sharing effect in JBS

The active cell of a JBS rectifier is shown in Fig. 1 and it consists of a device with two components: a vertical Schottky diode formed by the metal-semiconductor contact in the mesa of width m_W, and two vertical p-type wells with doping concentration N_a that form 2 lateral pn-junctions in the mesa region under the Schottky and 2 vertical pn-junctions with junction depth X_j. The drift region enhances the blocking voltage capability by supporting the applied bias in a thickness T_{epi} with n-type doping N_{epi}, whereas the substrate provides ohmic contact to back-side and mechanical handling.

Under forward bias or on-state, majority carriers are injected from the semiconductor into the metal by thermionic emission over the Schottky barrier and the current depends exponentially on the voltage [8]. The forward voltage drop V_F is directly proportional to the Schottky barrier height and the drift region resistance, which is determined by the thickness T_{epi} and doping N_{epi} of the layer. In addition, V_F is reduced in JBS devices because of the conductivity modulation of the mesa region due to minority carrier injection from the lateral pn-junction.

* Corresponding author.
E-mail addresses: adlatorr@asu.edu, alatorre@ieee.org (A.D. Latorre-Rey).

https://doi.org/10.1016/j.sse.2018.03.004
Received 31 October 2017; Received in revised form 7 March 2018; Accepted 7 March 2018
Available online 09 March 2018
0038-1101/

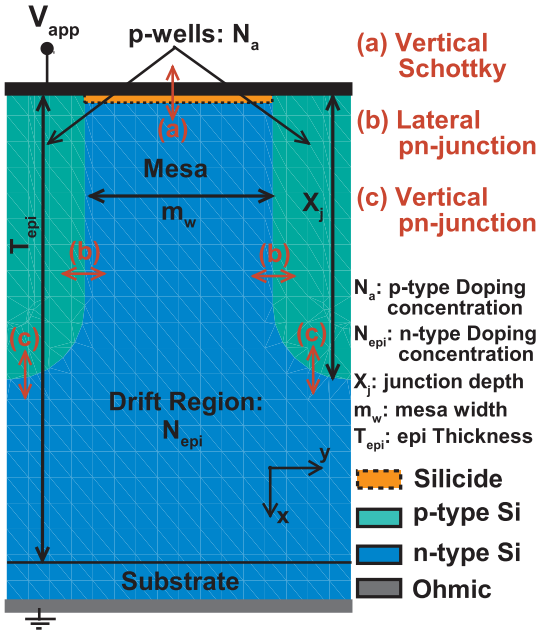

Fig. 1. Active cell of a JBS device showing the design parameters: mesa width m_W, junction depth X_j, p-type doping N_a, n-type epi doping N_{epi} and epi thickness T_{epi}.

Under reverse bias, the leakage current is due to the Schottky barrier height lowering effect which depends on the surface electric field [1], and the applied voltage is held by the drift region until the electric field reaches its critical value E_{crit} triggering avalanche breakdown by impact ionization, which can be reached either in the mesa or across the vertical pn-junctions. Avalanche breakdown was included in all our simulations through the impact-ionization generation rate model, where the impact ionization coefficients and its electric field dependence was calculated using the model by van Overstraeten [9]. Since the value of E_{crit} is a property of the material, the use of wide band gap semiconductors such as SiC and GaN intrinsically allow for higher breakdown voltages, however an additional tunneling current will contribute to the leakage which is not present in Si and therefore not included in our simulations.

Fig. 2(a) compares the reverse bias characteristics J_r–V_{app} of a planar Schottky and 2 JBS rectifiers showing the evident advantages of the JBS structure. When the drift region doping N_{epi} is kept constant, the JBS device (corresponding to curve JBS_1 in the figure) allows for higher breakdown voltage BV and lower leakage current density J_r than the planar counterpart, due to the reduction of the peak value and surface electric field respectively, which is an effect of adding the p-wells. Furthermore, the breakdown voltage of a planar Schottky can be matched by a JBS structure with higher doping N_{epi} as shown with curve JBS_2, with the advantage of providing lower leakage current and lower forward voltage V_F than the planar case.

Adding the pn-junction grid modulates the charge in the mesa region under the Schottky junction which reshapes the electric field profile in the device, particularly the vertical component (x-direction) along the drift region as shown in Fig. 2 (b) for V_{app} = 83 V, which corresponds to the breakdown voltage of the planar and JBS_2 devices. In the planar Schottky case the applied bias is supported with a triangular field distribution throughout regions (i)–(iii) in the figure, reaching the peak at the metal contact which is higher than the critical electric field E_{crit}, indicating breakdown of the junction.

Instead, for the device JBS_1 the electric field begins with a triangular distribution in region (iii) with the same slope as the planar case due to having the same N_{epi}, and then it changes slope in region (ii) suggesting an apparent inversion of the layer, reverting to its original sign close to the surface in region (i). In this case, the electric field is pushed into the drift region and, since the area under the electric field curves corresponds to the electrostatic potential which is equal to V_{app} = 83 V for both planar and JBS_1 devices, then the potential lost in regions (i) and (ii) is gained in the drift region (iii). Despite holding the same potential, the value of the electric field at the peak and at the surface for the JBS_1 is below E_{crit} and lower than the peak surface electric field for the planar case, which explains the higher breakdown voltage of V_{app} = 100 V as shown in Fig. 2(a), and lower leakage current respectively.

For a device with higher doping N_{epi} such as JBS_2 in Fig. 2(b), the vertical electric field profile has a steeper slope in region (iii) than the planar case reducing the potential gained. However, the reshaping of the electric field in regions (i) and (ii) is less pronounced than for the JBS_1, since the slope is only reduced without changing sign which produces a smaller potential lost resulting in the same total area of the planar Schottky and hence same BV. Even though the surface electric field in the mesa region corresponds to the peak field and it is above E_{crit}, its value is lower than the planar case which explains the lower leakage current for the same breakdown voltage observed in Fig. 2(a). For all cases under study region (iv) shows zero electric field because the devices reached breakdown before there was vertical punch-through from the drift region into the substrate.

The enhancement of breakdown voltage in JBS devices should be carefully studied because, unlike in the planar case, E_{crit} can be reached in the vertical pn-junctions instead of the drift region, which allows for optimization strategies for higher BV and lower leakage current J_r. This is illustrated in Fig. 3, where the vertical electric field profile along the

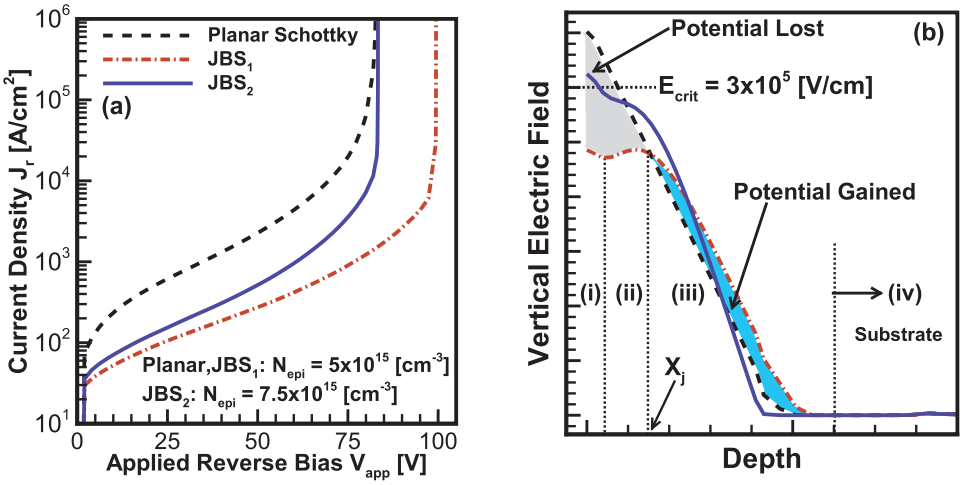

Fig. 2. Comparison of (a) IV curve under reverse bias and (b) vertical electric field along the mesa region of a planar Schottky and 2 JBS rectifiers at reverse bias V_{app} = 83 V.

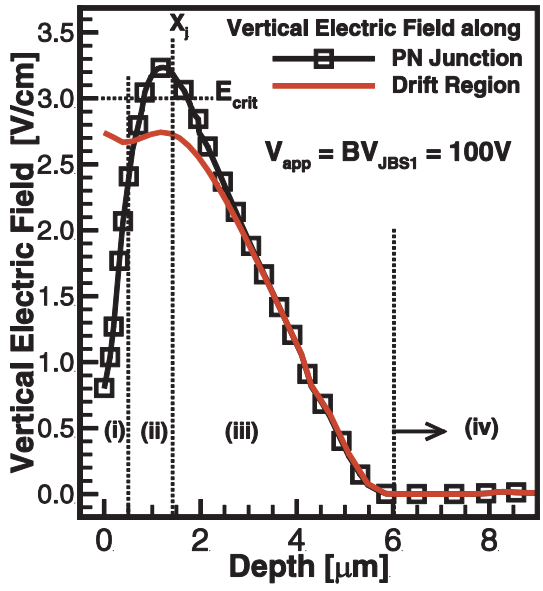

Fig. 3. Profile of the vertical electric field of device JBS_1 along pn-junctions (symbols) and along drift region (solid line) at V_{app} = 100 V.

drift region (solid line) and along the vertical pn-junction (symbols) of the JBS_1 is shown at V_{app} = 100 V which corresponds to its breakdown voltage. From the figure it can be seen that for the particular N_{epi} and p-well N_a doping conditions of this device, the peak electric field is reached along the pn-junction and it is higher than E_{crit}, whereas the field along the drift region is always below E_{crit}. This indicates that BV for the JBS_1 is limited by the vertical pn-junction. In general, the optimization of JBS devices is achieved when E_{crit} is simultaneously achieved along the drift-region and the vertical pn-junctions, which can be controlled with the doping concentrations N_{epi} and N_a.

The improved electrical characteristics of the JBS structure can be explained in terms of the charge-sharing effect as that observed in RESURF devices [10] and in Trench MOS Barrier Schottky rectifiers [11]. Fig. 4 shows a sketch of the depletion regions within the active cell and its progression as the applied reverse bias increases. At a given reverse bias V_{app1} as shown in Fig. 4(a), the depletion widths W_{Sch} and W_{pn} overlap in a region of the mesa, and the space charge provided by the doping N_{epi} is therefore shared between the two components. This translates into less available space charge in the mesa pushing the JBS depletion width deeper into the drift region as indicated by W_{JBS} in the figure.

As the applied voltage increases as shown in Fig. 4(b) for $V_{app2} > V_{app1}$, the lateral depletion regions W_{pn} merge while W_{Sch} also increases, in turn sharing all the area available in the mesa. From this point, any further increment in V_{app} causes the lateral punch-through as shown in Fig. 4(c), which couples the two lateral pn-junctions and further reduces the available space charge modulating the charge into an apparent inversion of the doping type.

The charge sharing effect between the vertical Schottky and the lateral pn-junctions in the mesa region is directly correlated to the electric field reshaping shown in Fig. 2(b) and therefore it explains the enhanced performance under reverse bias of the JBS device. Since the charge-sharing region expands as the applied bias V_{app} increases, the effective space charge available in the mesa to achieve charge neutrality condition decreases, producing bias dependent variations of the slope of the electric field that, from a modeling point of view, can be interpreted as an apparent inversion of doping type in the layer. Furthermore, in order to achieve charge neutrality the depletion width of the structure W_{JBS} is pushed into the drift region, redistributing the potential throughout the device and reducing the peak electric field which enables higher breakdown voltage capability. Finally, since most of the applied bias is held by the drift region there is a lower potential held close to the surface, which in turn reduces the surface electric field and yields lower leakage current due to a weaker Schottky barrier height lowering effect.

The term “apparent inversion” is used here to correlate the charge in the mesa region to the electric field profile of the JBS device which presents a change of slope, from negative in region (iii) to positive in region (ii), resembling a pn-junction like behavior as shown in Fig. 2(b). It is empirically derived from the charge-sharing analysis which indicates a progressive reduction of available space charge in the mesa region with bias. However, the inversion of the mesa is non-physical and the term “apparent” is added to distinguish it from the conventional use of inversion that describes the physical inversion of charge at the SiO_2/Si interface of a MOS device. In fact, even though the hole concentration in the depletion region is several orders of magnitude higher than in the drift region, due to the creation of electron-hole pairs through impact ionization and thermal generation, the hole concentration is not high enough to physically invert the layer. Despite being an empirical concept, the apparent inversion definition can be used to qualitatively explain the profile of the electric field, and also to derive an analytical equation for the effective charge as it is presented in Section 3, which allows calculating the electric field profile of these devices.

In terms of design strategies for JBS devices, the drift region doping N_{epi} offers important trade-offs between forward and reverse bias characteristics in terms of BV and V_F. This is studied in Fig. 5 where the extracted values of BV obtained with simulations of a planar Schottky and a JBS device with p-well doping $N_a = 5 \times 10^{16}$ cm^{-3} are shown as a function of N_{epi}. The highest BV for both structures is achieved at low

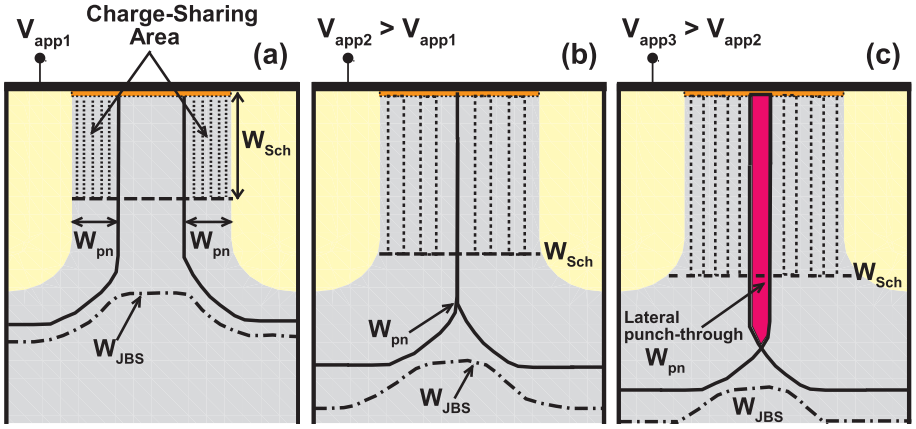

Fig. 4. Depletion widths of the Schottky W_{Sch}, pn-junction W_{pn} and the resulting JBS W_{JBS} due to the charge sharing effect at three different applied reverse bias conditions (a) V_{app1}, (b) $V_{app2} > V_{app1}$ and (c) $V_{app3} > V_{app2}$.

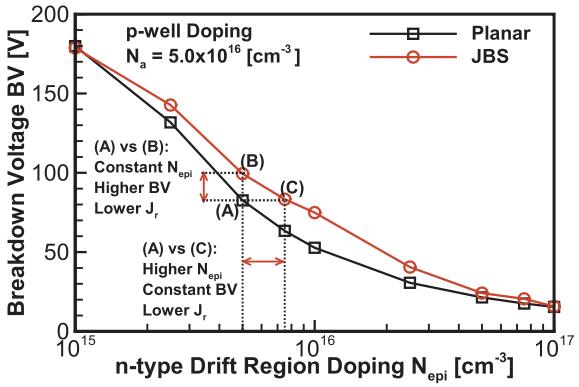

Fig. 5. Breakdown voltage BV as a function of n-type drift region doping N_{epi} for a Planar Schottky and a JBS device.

$N_{epi} = 10^{15}\,\mathrm{cm}^{-3}$ and as expected it decreases monotonically as N_{epi} increases. However, the BV in the JBS device is consistently higher than the planar due to the charge modulation in the mesa. The design trade-off is exemplified with points (A), (B) and (C) in Fig. 5 since structures (A) and (B) keep N_{epi} constant which translates into constant forward voltage but with the advantage of higher breakdown for the JBS. On the other hand, structures (A) and (C) result in the same breakdown voltage with the advantage for the JBS since a higher N_{epi} is used, therefore reducing the forward resistance which yields lower V_F while keeping lower leakage current than the planar device.

Regarding breakdown voltage BV and leakage current J_r optimization, due to the charge-sharing effect this is effectively done by varying the parameters that modulate the charge in the structure, such as the p-well doping which directly controls the depletion widths of the lateral pn-junctions in the mesa, while also determining the profile of the vertical electric field along the pn-junction which can be the limiting factor for BV in some designs. Fig. 6 shows the extracted values of BV and J_r as a function of p-well doping concentration N_a obtained with simulations of a JBS device where the cell pitch, drift region length and doping $N_{epi} = 2.5 \times 10^{15}\,\mathrm{cm}^{-3}$ were kept constant. The values of J_r correspond to the leakage current measured at a reverse bias of $V_{app} = 55$ V.

From the figure it can be seen that the breakdown voltage remains nearly constant for low N_a, and then it significantly increases and plateaus reaching a peak at $N_a = 2.6 \times 10^{16}\,\mathrm{cm}^{-3}$, to then monotonically decrease for higher values of N_a. The leakage current shows a different trend, since it first remains constant for low N_a, and then it consistently decreases as N_a increases, until it reaches a minimum value independent of the p-well doping. These trends can be explained in terms of the charge-sharing effect and the reshaping of the electric field profile.

For low values of $N_a < N_{epi}$ the charge sharing or anode shielding is

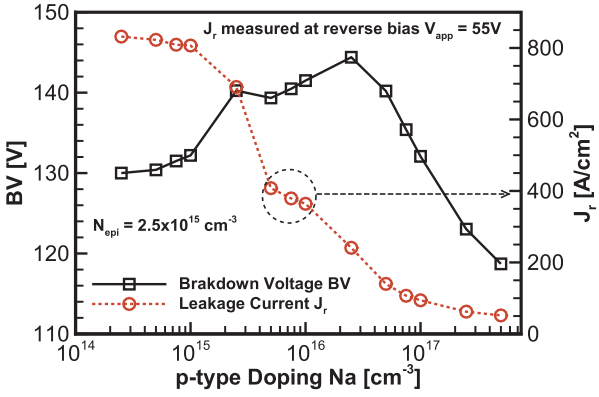

Fig. 6. Optimization of breakdown voltage BV (left y-axis) and reverse leakage current density J_r (right y-axis) as a function of p-well doping N_a.

weak and the BV and J_r show a slight improvement because the critical field is reached at the metal-semiconductor surface and the barrier height lowering is strong similar to the planar case. In contrast, for heavily doped p-wells where $N_a > 10^{17}\,\mathrm{cm}^{-3} \gg N_{epi}$ the charge modulation is strong evidenced by the low values of leakage current, which imply low surface electric field. However, in this case the peak electric field is located along the vertical p^+n-junction instead of along the drift region and it reaches E_{crit} at a lower applied bias than the mesa, limiting the breakdown voltage. Finally, the optimum BV while keeping low J_r for this design is achieved in the range of $N_a = 2.6 \times 10^{15}$ and $5 \times 10^{16}\,\mathrm{cm}^{-3}$ which provides moderate charge-sharing, and the electric field along the mesa and across the vertical pn-junction reach the critical value E_{crit} simultaneously [11].

3. Charge based model

In order to develop a model for the electric field profile, we determine the shared charge between the vertical Schottky junction and the lateral pn-junctions in the mesa region under the Schottky by calculating each charge component separately and then combining the effects into the JBS structure applying the principle of superposition. In all our derivations, the convention for reverse bias is $V_{app} < 0$, which corresponds to a grounded cathode and the bias applied to the anode.

Under reverse bias, the charge provided by the depletion region of the vertical Schottky in the mesa region away from the lateral pn-junctions is given by:

$$Q_{sch} = qN_{epi}W_{sch} \tag{1}$$

where the Schottky depletion width W_{sch} is defined as

$$W_{sch} = \sqrt{2k_s\varepsilon_0\frac{(V_{bi\_Sch} - V_{app})}{qN_{epi}}} \tag{2}$$

so that V_{bi_Sch} is the Schottky built-in potential, and constants k_s and ε_0 represent the relative permittivity of silicon and the permittivity of vacuum respectively.

However, due to the depletion region overlap with that of the lateral pn-junctions, the available charge for the Schottky junction is reduced by a factor ΔQ_{sch} given by

$$\Delta Q_{sch} = qN_{epi}W_{sch}\cdot 2W_{pn}/m_W = Q_{sch}\cdot\eta_{sch} \tag{3}$$

where η_{sch} is the charge-sharing efficiency factor and W_{pn} is defined as:

$$W_{pn} = \sqrt[3]{12k_s\varepsilon_0\frac{(V_{bi\_pn} - V_{app})}{q\cdot\sigma}} \tag{4}$$

where the linearly graded pn-junction approximation has been used in (4) to take into account the gradient in the doping profile due to the lateral out-diffusion, then V_{bi_pn} is the pn-junction built in potential and σ corresponds to the slope of the doping profile so that $N_{epi} - N_a = \sigma\cdot y$, where y is the position along the lateral component of the device. In the case of an abrupt single sided p^+n-junction, Eq. (4) should be replaced by the typical depletion width equation given by $W_{pn} = (2\kappa_s\,\epsilon_o/(q\cdot N_{epi})\cdot(V_{bi} - V_r))^{1/2}$ in the remaining derivation.

Next, taking into account the reduction in charge due to the sharing, the effective charge available in the mesa region under the vertical Schottky junction is therefore given by:

$$Q_{Eff} = Q_{sch} - \Delta Q_{sch} = Q_{sch}(1 - \eta_{sch}) \tag{5}$$

where η_{sch} is a measure of the degree of charge sharing in the mesa region, and it depends on the doping concentration N_a, the rate of change of doping σ and the mesa width m_W. It must be pointed out that Eq. (5) is only valid for the region of the mesa within the pn-junctions identified as region (ii) throughout the manuscript.

Fig. 7 shows a plot of the space charge in the mesa region considering the case of an isolated vertical Schottky given by (1) and the effective charge in a JBS device calculated with (5). It is evident from

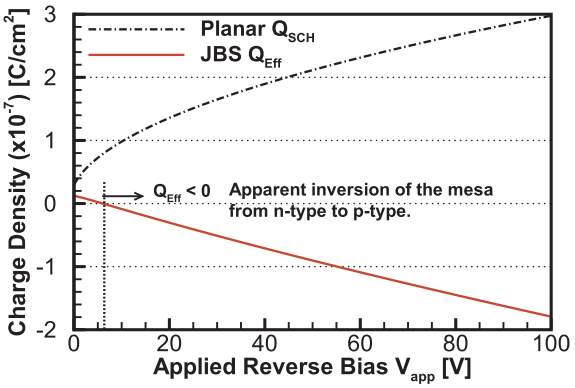

Fig. 7. Depletion charge as a function of applied reverse bias for a planar Schottky device Q_{Sch} and the effective charge for the JBS device Q_{Eff} due to the charge sharing, calculated with eq. (5).

(3) that as V_{app} increases η_{sch} also increases due to the lateral depletion region width W_{pn} which reduces the effective charge as shown in the figure. Furthermore, at high enough V_{app} the effective charge available for the Schottky junction changes sign according to (5) which models the apparent inversion of the layer from n-type to p-type responsible of the reshaping and reduction of the vertical electric field in the mesa region.

It should be highlighted that in the derivation of Eq. (5), the inversion of the effective charge is not imposed. On the contrary, it is naturally obtained by applying the principle of superposition of the decoupled charge neutrality condition of the vertical Schottky and the lateral pn-junctions. Since the behavior of Q_{Eff} shows that as the reverse bias increases there is a change of sign in the charge, this justifies the non-conventional use of the term "apparent inversion".

With the aim of deriving 1-D equations for the vertical electrical field along the drift region in the middle of the mesa ($y = m_w/2$), a piecewise approach similar to the used for typical p-n or p-i-n diodes is chosen where four regions can be identified (as shown in Fig. 2(b)): region (i) near the Schottky surface within the equilibrium depletion width $W_{Sch\_Eq} = W_{Sch}|_{V_{app}=0}$, region (ii) from W_{Sch_Eq} to the bottom of the p-wells given by the junction depth X_j where most of the sharing takes place suppressing the electric field, region (iii) from X_j to the bottom of drift region with length T_{epi} and a fourth region (iv) if the device goes into vertical punch-through into the substrate with high doping N_{sub}.

Next, a charge density can be defined for each region taking into account the charge-sharing effect as modeled by Eqs. (1)–(5) as follows:

$$\rho_i = qN_{epi}\cdot\alpha_{coupling} \tag{6}$$

$$\rho_{ii} = \rho_{Eff}\cdot\alpha_{coupling} = qN_{epi}(1-\eta_{sch})\cdot\alpha_{coupling} \tag{7}$$

$$\rho_{iii} = qN_{epi} \tag{8}$$

$$\rho_{iv} = qN_{Sub} \tag{9}$$

where $\alpha_{coupling}$ is a dimensionless factor that accounts for the additional reduction of available depletion charge due to the lateral punch-through of the 2 lateral pn-junctions.

Under lateral punch-through $W_{pn} > m_W/2$ as shown in Fig. 4(c), which allows to define an overlapping efficiency factor $\eta_{overlap} = (W_{pn}-m_W/2)/W_{pn} = 1-m_W/(2W_{pn})$. Then, the available space charge is reduced by a factor $\Delta Q_{over} = Q\eta_{overlap}$, yielding an available space charge $Q_{over} = Q-\Delta Q_{over} = Qm_W/(2W_{pn})$. This can be interpreted as a the available charge being reduced by a coupling factor $\alpha_{coupling} = m_W/(2W_{pn})$, which is only valid under lateral punch-through. In order to extend the range of validity of $\alpha_{coupling}$ to when there is no overlapping $W_{pn} < m_W/2$, the coupling factor is modified to impose $\alpha_{coupling} = 1$ before lateral punch-through to reflect the fact that there is no additional reduction of charge. The final form of the coupling factor is then given by:

$$\alpha_{coupling} = \frac{\min[m_w,\, 2W_{pn}]}{2W_{pn}} \tag{10}$$

where $min[a,b]$ refers to the function that returns the minimum value between [a,b]. From eq. (10) it can be seen that $\alpha_{coupling} = 1$ for $W_{pn} \leqslant m_W/2$ which corresponds to the condition before lateral punch-through. For $W_{pn} > m_W/2$ its value decreases with V_{app} and it goes from 1 to 0.5 when $W_{pn} = m_W$, which is reached at very low bias, therefore assuming $\alpha_{coupling} = 0.5$ for high V_{app} is a reasonable approximation.

Even though the overlapping of the space charge regions of the 2 lateral pn-junctions and the derivation of the coupling factor are physical, some effects have been neglected such as considering the curvature of the junctions as well as the condition $W_{PN} \gg m_W$. In this sense the factor $\alpha_{coupling}$ can be considered as semi-empirical. Nevertheless, it is necessary to include it because if the effect of lateral punch-through was neglected, the calculated charge would be significantly overestimated yielding inaccurate electric field profiles, particularly at the metal-semiconductor surface. Concerning the validity of the charge density definitions given by Eqs. (6)–(9), it must be noticed that in (6) the vertical Schottky component was assumed to be dominant close to the surface allowing to neglect the effect of charge-sharing before lateral punch-through. Also, the cylindrical junction effect at the bottom of the p-wells has been neglected which is valid for large radii.

Finally, thanks to the charge-sharing effect modeling given by Eqs. (6)–(9), the tedious 2-D electrostatic problem was reduced to the simple 1-D case of Gauss' Law and the electric field along the mesa of the JBS can be analytically calculated in each region as:

$$E_{i,\ldots,iv}(x) = \int_{x1}^{x2} \frac{\rho_{i,\ldots,iv}}{k_s\varepsilon_0}\,dx \tag{11}$$

where $x1$ and $x2$ determine the location of the boundary conditions so that the electric field is continuous throughout the device, i.e. $(E_i = E_{ii})|_{W_{Sch\_Eq}}$, $(E_{ii} = E_{iii})|_{X_j}$ and $(E_{iii} = E_{iv})|_{T_{epi}}$.

Applying eq. (11) to each region with the corresponding charge density, the full analytical expressions for the vertical electric field can be written as follows:

$$E_{i,\ldots,iv}(x) = \begin{cases} -\frac{\rho_i}{\epsilon_s}\cdot(x_{nI}-x), & \text{(i) for } 0 < x < x_{nI0} \\ -\frac{\rho_{ii}}{\epsilon_s}\cdot(x_{nI0}+x_{nII}-x), & \text{(ii) for } x_{nI0} < x < X_j \\ -\frac{\rho_{iii}}{\epsilon_s}\cdot(X_j+x_{nIII}-x), & \text{(iii) for } X_j < x < T_{epi} \\ -\frac{\rho_{iv}}{\epsilon_s}\cdot(T_{epi}+x_{nIV}-x), & \text{(iv) for } T_{epi} < x \end{cases} \tag{12}$$

where x_{nI0} corresponds to the length of region I close to the surface where no charge-sharing is present, and variables x_{nI} to x_{nIV} are derived from the boundary conditions and are given by:

$$x_{nI0,\ldots,IV} = \begin{cases} x_{nI0} = W_{Sch}(V_{app}=0) = \sqrt{2k_s\varepsilon_0\frac{(V_{bi-Sch})}{qN_{epi}}} \\ x_{nI} = W_{Sch} = \sqrt{2k_s\varepsilon_0\frac{(V_{bi-Sch}-V_{app})}{qN_{epi}}} \\ x_{nII} = \frac{\rho_i}{\rho_{ii}}\cdot(x_{nI}-x_{nI0}) \\ x_{nIII} = \frac{\rho_{ii}}{\rho_{iii}}\cdot(x_{nI0}+x_{nII}-X_j) \\ x_{nIV} = \frac{\rho_{iii}}{\rho_{iv}}\cdot(X_j+x_{nIII}-T_{epi}) \end{cases} \tag{13}$$

A quick inspection of Eqs. (12) and (13) indicates that the electric field as derived here shows a simple linear dependency with depth due the 1-D modeling of the charge density distributions. Also, all relevant design parameters of a JBS such as m_W, X_j, N_a, N_{epi} and T_{epi} are clearly preserved in the expressions. In particular the effect of the mesa width and the p-well doping, responsible for the reshaping and reduction of the electric field, is readily captured through the charge-sharing efficiency factor η_{sch}.

Finally, the validation of the model is presented in Fig. 8 where

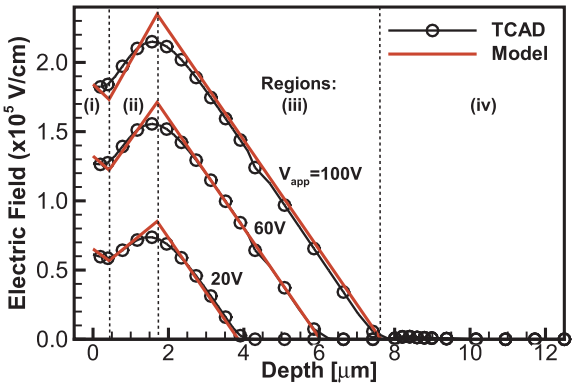

Fig. 8. Comparison of the Electric field along the mesa of a JBS device obtained with the proposed analytical model and TCAD simulations for applied reverse bias of 20, 60 and 100 V.

simulated electric field profiles obtained with TCAD are compared with the calculated values using the analytical model given by Eqs. (12) and (13), showing good agreement throughout all regions of interest of the device at three different values of V_{app}. It must be noticed that despite the 1-D nature of the charge-sharing concept, the model predicts the values of the surface and peak electric field with reasonable accuracy while preserving physical insight in the mathematical expressions, capturing the main variables that determine the performance of JBS rectifiers. This quality can be exploited in the design and optimization of JBS rectifiers.

4. Conclusion

A novel charge-based model for Junction Barrier Schottky (JBS) diodes has been presented, where simple analytical equations of the electric field profile along the mesa of the device were derived. Instead of solving the 2-D poisson equation, the method relies on modeling the charge distribution in the mesa region under the Schottky by means of the charge-sharing effect between the vertical Schottky junction and the lateral pn-junctions that constitute the active cell of the device. Using this concept, a qualitative description of the JBS operation was presented along with a brief description of breakdown voltage and leakage current optimization strategies. Then the detail derivation of the equations was shown, followed by the model validation performed by comparing drift-diffusion simulations of a JBS device with calculated electric field profiles showing good agreement. The main advantage of the proposed model is that with simple 1-D expressions, it is possible to capture the reshaping and reduction of the electric field profile responsible for the improved electrical performance of these devices, while preserving physically meaningful expressions that depend on relevant device parameters which can be exploited in device design and optimization.

References

[1] Baliga BJ. Fundamentals of power semiconductor devices. Springer Science & Business Media; 2010.
[2] Baliga BJ. The pinch rectifier: a low-forward-drop high-speed power diode. IEEE Trans Electron Dev 1984;5(6):194–6.
[3] Tone K, Zhao JH, Weiner M, Pan M. 4H-SiC junction-barrier Schottky diodes with high forward current densities. Semicond Sci Technol 2001;16(7):594.
[4] Li W, Nomoto K, Pilla M, Pan M, Gao X, Jena D, et al. Design and realization of GaN trench Junction-Barrier-Schottky-Diodes. IEEE Trans Electron Dev 2017;64(4):1635–41.
[5] Baliga BJ. Analysis of Junction-Barrier-Controlled Schottky (JBS) rectifier characteristics. Solid-State Electron 1985;28(11):1089–93.
[6] Radhakrishnan R, Zhao J. A 2-dimensional fully analytical model for design of high voltage junction barrier Schottky (JBS) diodes. Solid-State Electron 2011;63(1):167–76.
[7] Ren N, Sheng K. An analytical model with 2-D effects for 4H-SiC trenched Junction Barrier Schottky diodes. IEEE Trans Electron Dev 2014;61(12):4158–65.
[8] Sze SM, Ng KK. Physics of semiconductor devices. John Wiley & Sons; 2006.
[9] Van Overstraeten R, De Man H. Measurement of the ionization rates in diffused silicon pn junctions. Solid-State Electron 1970;13(5):583–608.
[10] Imam M, Quddus MT, Adams J, Hossain Z. Efficacy of charge sharing in reshaping the surface electric field in high-voltage lateral RESURF devices. IEEE Trans Electron Dev 2004;51(1):141–8.
[11] Latorre-Rey AD, Mudholkar M, Quddus MT. Physics based breakdown voltage optimization of trench MOS Barrier Schottky rectifiers. IEEE Trans Electron Dev 2018;65(3):1–7.

Alvaro D. Latorre-Rey (S'09-M'17) was born in Caracas, Venezuela. He received the Professional Electronics Engineering (Cum Laude) degree in 2009 and the Magister of Electronics Engineering (Honors) degree, with a major in solid-state electronics, in 2011, both from Universidad Simon Bolivar, Caracas-Venezuela. He is currently working towards the PhD degree in the Arizona State University in Tempe, within the Center for Computational Nanoscience. From May to December 2017 he held an internship at ON Semiconductor Corporation within the Power Solutions Group. His research interests are in the field of design, simulation (Monte Carlo and drift-diffusion), physics-based modeling and characterization of RF and power semiconductor devices such as GaN HEMTs, MOSFETs and diodes in Si and SiC. He is an IEEE Eta Kappa Nu member and a coauthor of several articles published in technical journals and specialized conferences.

Mihir Mudholkar (S'06-M'13) received his B.Tech degree in Electrical Engineering from IIT Kanpur, Kanpur, India, in 2006, and his Ph.D. degree in Electrical Engineering from University of Arkansas, Fayetteville, AR, USA, in 2012. His Ph.D. research was focused on characterization and modeling of low voltage and high voltage silicon carbide MOSFETs for power applications. He is currently working with the Power Solutions Group at ON Semiconductor in Phoenix, AZ, USA, where his work is focused on the design and development of SiC MOSFETs and trench-based Si Schottky diodes. His research interests include design and modeling of wide band-gap power devices including MOSFETs, didoes and IGBTs. He has co-authored over 20 peer-reviewed journal and conference papers, and has more than 10 patents and pending patents in the area of semiconductor device design and modeling.

Mohammed Tanvir Quddus received his B.Sc and M.Sc in Electrical Engineering from BUET (Bangladesh University of Engineering and Technology) in 1991 and 1993 respectively. He served as a faculty member of the Department of Electrical and Electronic Engineering of BUET from 1991 to 1995. He received his Ph.D. from ASU (Arizona State University) of Tempe, USA, in December 1999. From 1991 till 1999 he was mainly engaged in modelling and characterization of small geometry MOS devices. In 2000, he joined ON Semiconductor, Phoenix, USA. Since then he was extensively involved in power device development involving different Discrete and IC technologies. He is a senior member of IEEE. He has authored and co-authored 17 papers in various scientific journals and conferences. He holds 26 issued, 3 pending and 4 new applications to be filed.

Ali Salih received his B.S. degree (honors) in Physics, his M.S. degree in Solid-State Physics, and his Ph.D. degree in Electronic Materials Science and Engineering (with a minor in electrical engineering), all from North Carolina State University. He is the senior director of the Technology Development for the Standard Products Group of ON Semiconductor, Phoenix, Arizona. He has a long career in the semiconductor industry with 30 years of experience in power device design and new product development. He is responsible for the development of IGBTs, MOSFET, rectifiers, wide band gap, and small signal devices. He has spent most of his career at ON Semiconductor (formerly a group of Motorola), where his responsibility covered all classes of power semiconductor devices. He has published over 50 papers, presented in technical conferences, and has 28 issued patents to his credit.